

## Responses to Anonymous Referee #1

We thank the Anonymous Referee #1 for their time and effort to review our revised manuscript, which helped to further increase the quality of the paper. All comments have been addressed carefully.

Below, reviewer comments are marked in **red**.

Responses to the comments are marked in **blue**.

Changes that have been made in the manuscript are marked in *italic*.

### Comments

The authors partially addressed my comments. But, I still have some concerns which is mainly about the consistency evaluation and assessment.

1) The sharp increase of VOD C<sub>XKu</sub> in 1992 coincides with the introduction of a new sensor, SSMI F11. Is it caused by the unresolved bias among sensors? Similar trend can be observed with the 2003 decrease (coinciding with the introduction of AMSR-E), and the 2012 increase (coinciding with the introduction of AMSR2). Please explain it

We thank the reviewer for this important question concerning the continuity of VODCA C<sub>XKu</sub>.

- Regarding the SSM/I sensors, VOD (and soil moisture) observations were retrieved from the GPM SSMI Common Calibrated Brightness Temperatures L1C produced by NASA (Berg, 2021). This L1C dataset provides recalibrated brightness temperatures for the SSM/I sensors using a common basis (GPM GMI brightness temperature) to enable retrievals of consistent datasets for the entire SSM/I period (Berg et al., 2016, 2018; Berg, 2021). This dataset is part of the Fundamental Climate Data Record (FCDR) of brightness temperatures (T<sub>b</sub>) and provides, according to NASA, the best intercalibration of SSM/I sensors available (Berg et al., 2018). In the VODCA framework, we, therefore, concatenate the VOD retrievals from SSM/I F8, F11, and F13 into a single record without further inter-calibration at the VOD level. As F8 and F11 do not overlap with each other or any other radiometer used in the VODCA framework, further intercalibration and validation steps are challenging and thus we rely on the FCDR as provided by NASA. The patterns in VODCA C<sub>XKu</sub> are fully compliant with patterns observed in the single-frequency VODCA v1 Ku-band, both in terms of global anomaly time-series (Dorigo et al. (2021), Fig. SB2.6) and latitude-longitude anomalies Moesinger et al. (2020), Fig. 6), indicating they are not a result of combining multiple frequencies. There are no independent VOD datasets covering the period before 1992 that could serve as validation data. Additionally, all optical-based vegetation datasets available before 1992 are multi-sensor products, such as those using the Advanced Very High Resolution Radiometer (AVHRR) sensors onboard NOAA, which are known to have their own (inter)calibration issues (Brown et al., 2006; Tian et al., 2015); therefore, their usage for this type of evaluation is questionable. In conclusion, we cannot exclude sensor intercalibration issues between SSM/I F8 and F11. We will modify the text to make the users aware of this possible issue. Potential intercalibration issues between SSM/I F8 and F11 originate from the brightness temperature calibration and not from the VODCA framework.
- To analyse the plausibility of the observed VODCA patterns, such as the decrease in 2003 and the increase in 2012, we computed global time series of yearly fAPAR (Fig. 1), as well as a

Hovmoeller diagram of monthly fAPAR anomalies (Fig. 2) using MODIS fAPAR data (Myneni and Park, 2021), which is a single-sensor dataset. We can observe a decrease in global yearly fAPAR in 2003 and an increase in 2012. Similar patterns can be observed in the Hovmoeller diagram, particularly in the Southern Hemisphere. Additionally, these patterns of decrease in 2003 are even more visible in the Hovmoeller plot showing MODIS LAI anomalies, presented in (Moesinger et al., 2020) in Fig. 6. We therefore strongly believe that the patterns mentioned by the reviewer are plausible and we attribute them to natural variability.

*Fig. 1 will be added to the Annex. SSM/I information on brightness temperature calibration will be added to Chapter 2.1.2 "Passive microwave data". Information about the concatenation of SSM/I will be added to Chapter 3.2 "Preprocessing". The patterns mentioned by the reviewer (1992, 2003, 2012) are discussed in Chapter 4.2 "Spatio-temporal consistency". We mention that we cannot exclude an intercalibration issue between F08 and F11 in Chapter 4.2 "Spatio-temporal consistency" and in Chapter 5 "Conclusion".*

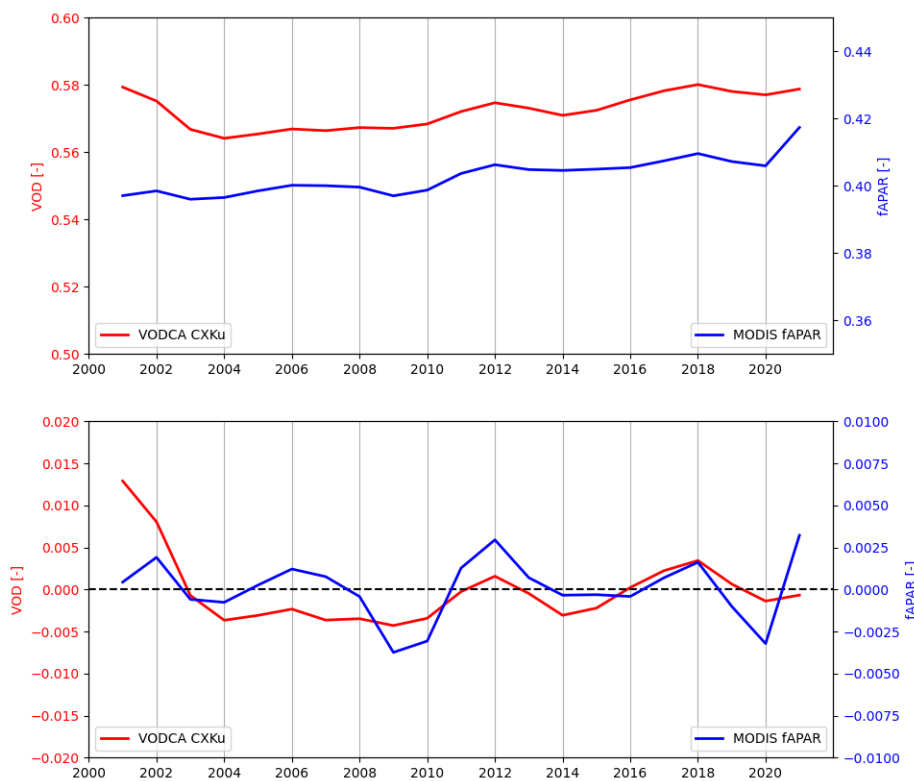


Figure 1: Yearly global time-series of VODCA CXKu and fAPAR for the bulk signal (upper graphic) and for anomalies (lower graphic).

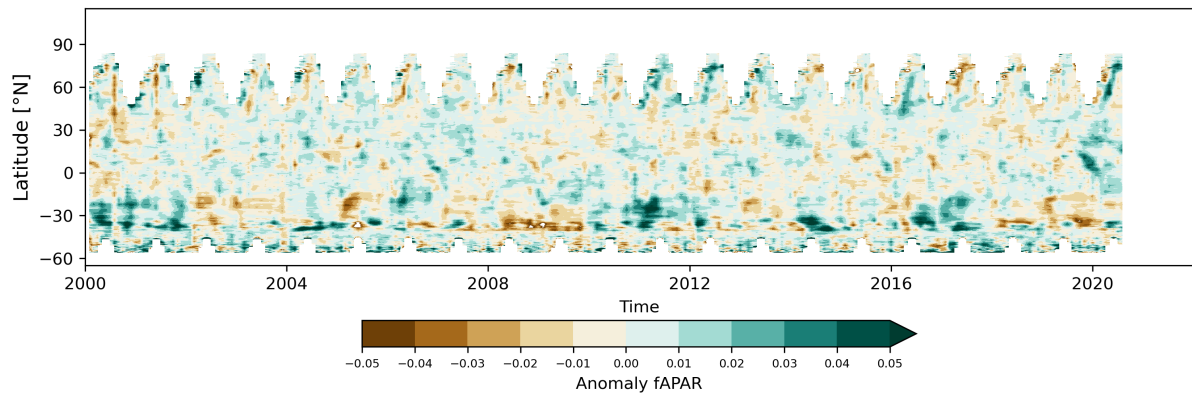


Figure 2: Hovmöller diagrams showing anomalies of the monthly means per latitude for MODIS fAPAR.

2) Figure A5 & A6 should be placed in the main text than Figure 5 & 6. Because the monthly variations in Figure 5 & 6 make the system bias less noticeable. Readers need to use the yearly time series to assess the consistency.

We moved the Figures A5 and A6 to the main text body.

*Figures A5 and A6 will be moved to Figure 5 and 6 in Chapter 4.2 "Spatio-temporal consistency".*

3) In my previous review, I requested the inclusion of yearly time series for VOD products at continental or land cover scales. However, these results were not included. For this round, please add the yearly time series VOD specifically for tropical and boreal forests.

We apologize for the misunderstanding, we did not mean to omit providing continental or landcover time-series. From the formulation in the initial request ("at global, continental, or landcover scales.") we understood that the reviewer lets the authors decide which type of time-series to provide, so we provided global and hemisphere plots. We gladly provide the landcover and continental plots in this iteration. As in this iteration the reviewer asked specifically for tropical forests, we refer to the BEF class in the landcover time-series plot. To isolate boreal forest, we created time-series plots for the *Dfc* Koeppen-Geiger climate classification (Kottek et al., 2006). We also provide fAPAR time-series for comparison with VODCA CXKu and SMOS IC VOD time-series for comparison with VODCA L.

*We provide the time series per landcover (Figs. 3, 4), per continent (Figs. 7, 8) and for the Dfc climate class corresponding to boreal forest (Figs. 5, 6) in the Annex.*

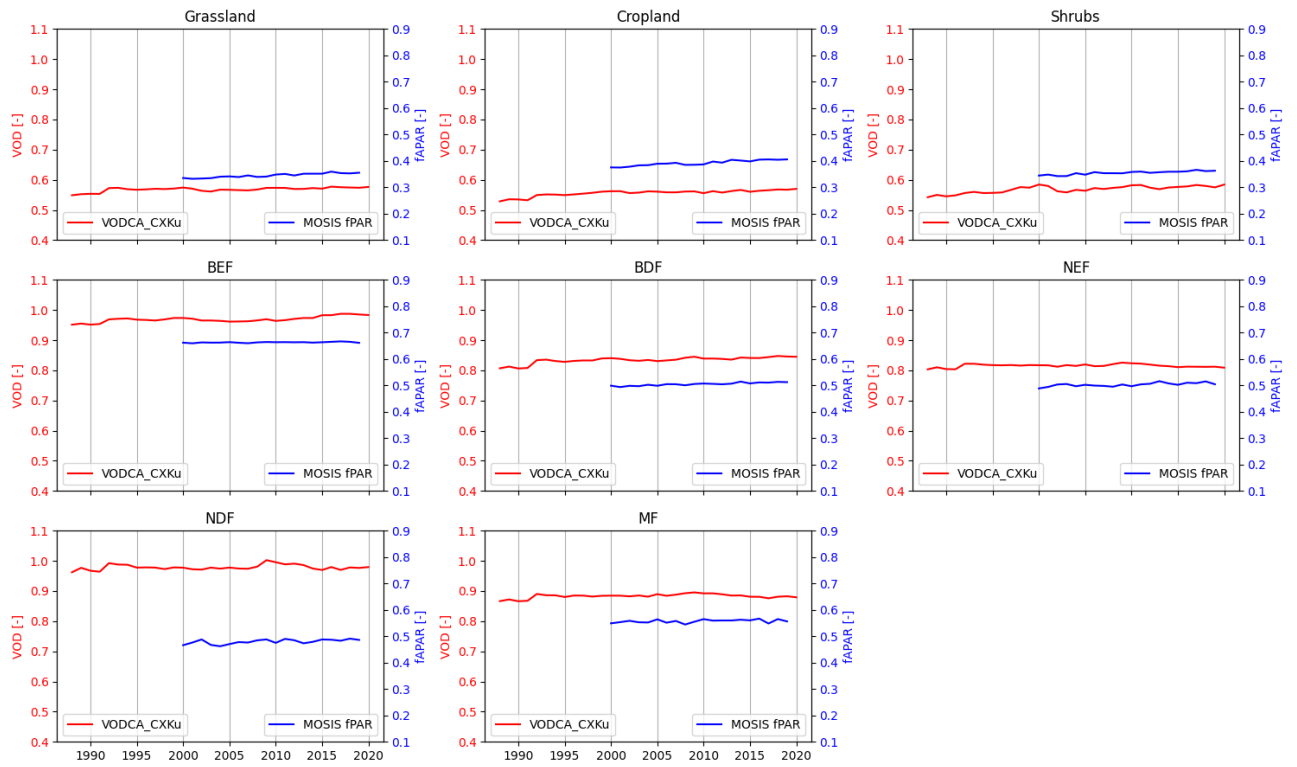


Figure 3: Time-series per landcover class for VODCA CXKu and MODIS fPAR. ESA CCI LC was used.

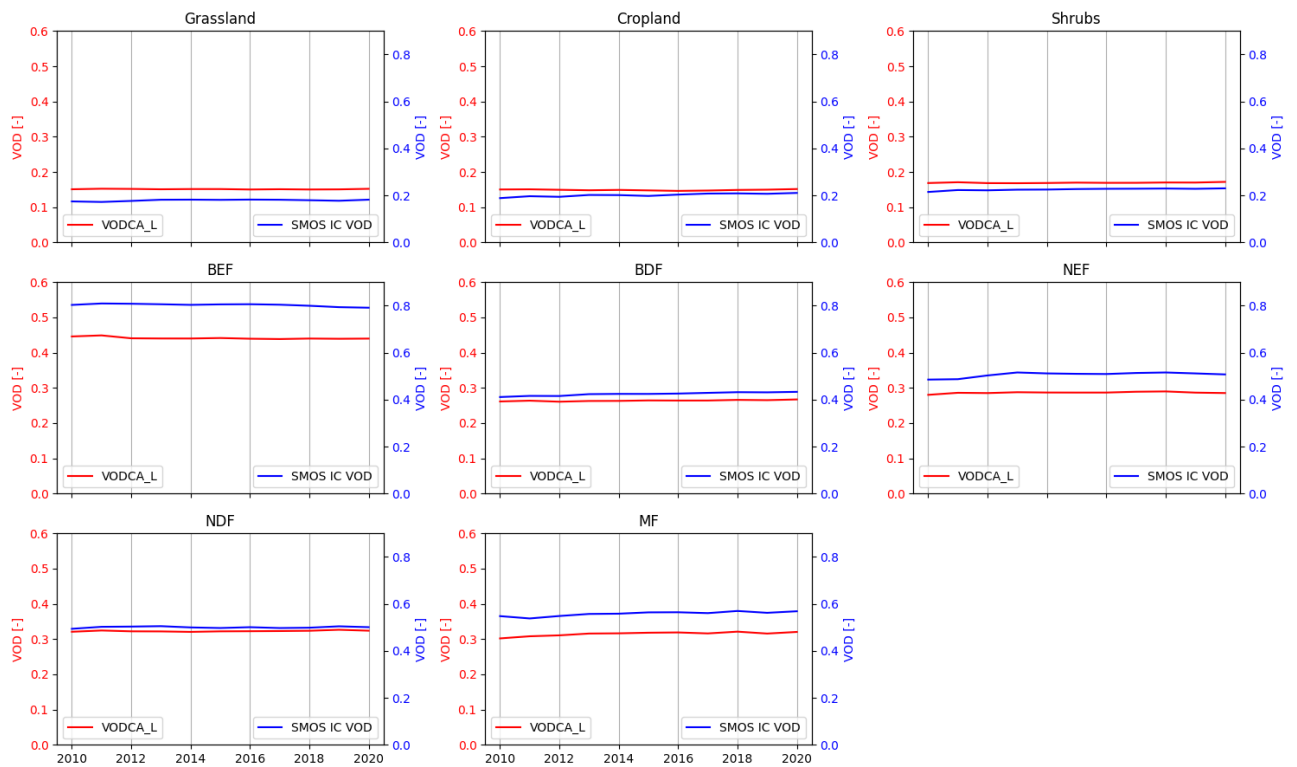


Figure 4: Time-series per landcover class for VODCA L and SMOS IC VOD. ESA CCI LC was used.

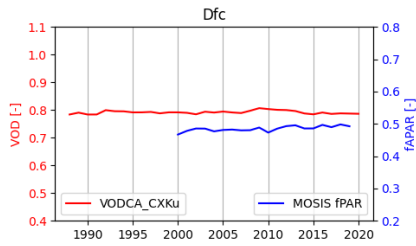


Figure 5: Time-series for the Dfc climate, corresponding to boreal forest, for VODCA CXKu and MODIS fPAR.

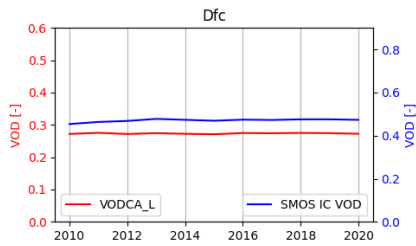


Figure 6: Time-series for the Dfc climate, corresponding to boreal forest, for VODCA L and SMOS IC VOD.

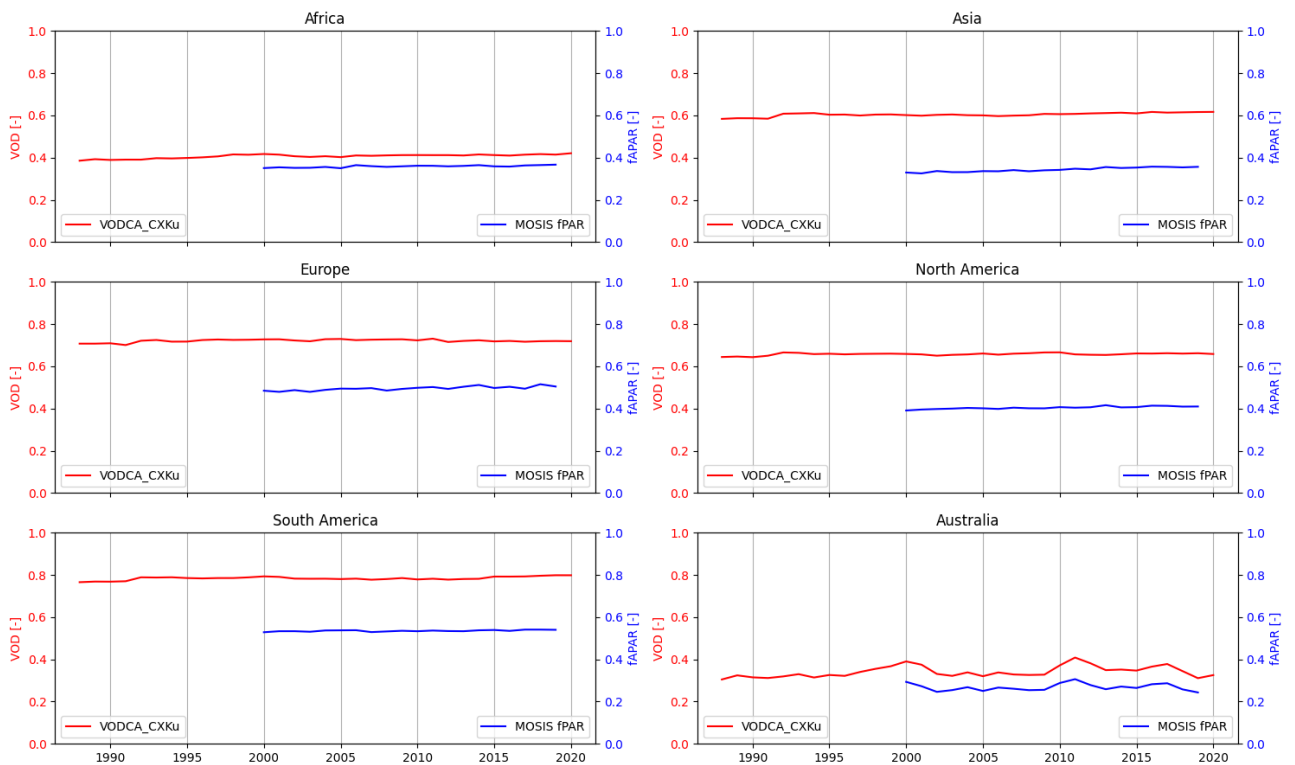


Figure 7: Time-series per continent for VODCA CXKu and MODIS fPAR.

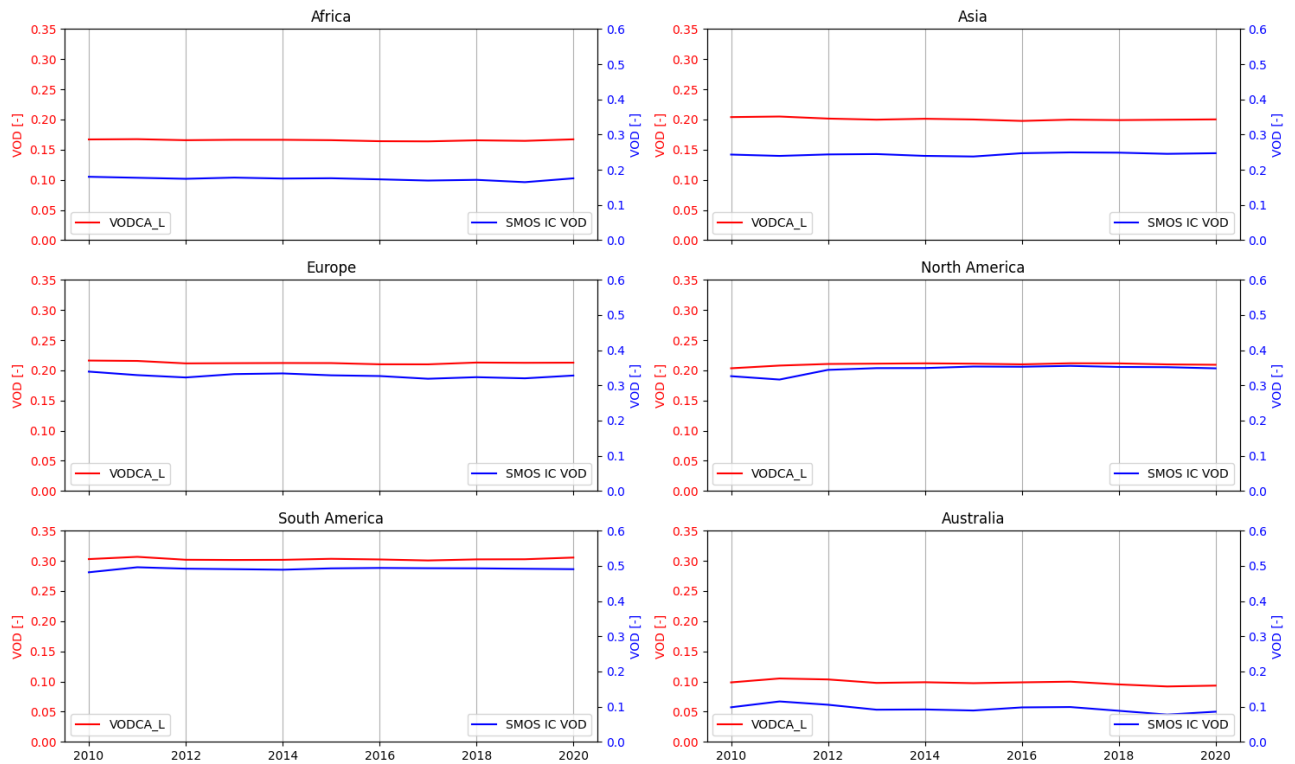


Figure 8: Time-series per continent for VODCA L and SMOS IC VOD.

## References

- Berg, W.: GPM SSM/I on F08 Common Calibrated Brightness Temperatures L1C 1.5 hours 13 km V07, Greenbelt, MD, USA, Goddard Earth Sciences Data and Information Services Center (GES DISC), 2021.
- Berg, W., Bilanow, S., Chen, R., Datta, S., Draper, D., Ebrahimi, H., Farrar, S., Jones, W. L., Kroodsma, R., McKague, D., et al.: Intercalibration of the GPM microwave radiometer constellation, *Journal of Atmospheric and Oceanic Technology*, 33, 2639–2654, 2016.
- Berg, W., Kroodsma, R., Kummerow, C. D., and McKague, D. S.: Fundamental climate data records of microwave brightness temperatures, *Remote Sensing*, 10, 1306, 2018.
- Brown, M. E., Pinzón, J. E., Didan, K., Morisette, J. T., and Tucker, C. J.: Evaluation of the consistency of long-term NDVI time series derived from AVHRR, SPOT-vegetation, SeaWiFS, MODIS, and Landsat ETM+ sensors, *IEEE Transactions on geoscience and remote sensing*, 44, 1787–1793, 2006.
- Dorigo, W., Möisinger, L., van der Schalie, R., Zotta, R.-M., Scanlon, T. M., and De Jeu, R.: Long-term monitoring of vegetation state through passive microwave satellites [in “State of the Climate in 2020”], *Bulletin of the American Meteorological Society*, 102, S110–S112, 2021.
- Kottek, M., Grieser, J., Beck, C., Rudolf, B., and Rubel, F.: World map of the Köppen-Geiger climate classification updated, 2006.
- Moesinger, L., Dorigo, W., de Jeu, R., van der Schalie, R., Scanlon, T., Teubner, I., and Forkel, M.: The global long-term microwave vegetation optical depth climate archive (VODCA), *Earth System Science Data*, 12, 177–196, 2020.

Myneni, R. and Park, T.: MODIS/Terra+ Aqua Leaf Area Index/FPAR 4-Day L4 Global 500 m SIN Grid V061, The Land Processes Distributed Active Archive Center (LP DAAC): Sioux Falls, SD, USA, 2021.

Tian, F., Fensholt, R., Verbesselt, J., Grogan, K., Horion, S., and Wang, Y.: Evaluating temporal consistency of long-term global NDVI datasets for trend analysis, *Remote Sensing of Environment*, 163, 326–340, 2015.

## Responses to Anonymous Referee #2

We thank the Anonymous Referee #1 for their time and effort to review our revised manuscript, which helped to further increase the quality of the paper. All comments have been addressed carefully.

Below, reviewer comments are marked in red.

Responses to the comments are marked in blue.

Changes that have been made in the manuscript are marked in *italic*.

### Comments

Thank you to the authors for their efforts; they have addressed most of my concerns. However, I still have a concern regarding the Hovmöller diagrams in Figure 6. Why is the VODCA CXK anomaly significantly lower and showing gaps during the period from 1988 to 1992? Could this be due to imperfections in the data fusion process? The decrease in 2003 (coinciding with the introduction of AMSR-E) and the increase in 2012 (coinciding with the introduction of AMSR2) also show similar trends. Please explain.

We thank the reviewer for these important questions. Regarding the 1988 to 1992 period, we mention that there are no data gaps; we mistakenly cut out values below -0.05 in the graphic. We corrected that as seen in Fig. 1. There are indeed lower anomalies in the period before 1992, and hence between SSM/I F8 and F11. We mention that the data producers intercalibrated the SSM/I sensors at the brightness temperature level. VOD (and soil moisture) observations were retrieved from the GPM SSM/I Common Calibrated Brightness Temperatures L1C produced by NASA (Berg, 2021). The L1C dataset provides recalibrated brightness temperatures for the SSM/I sensors using a common basis (GPM GMI brightness temperature) to enable retrievals of consistent datasets for the entire SSM/I period (Berg et al., 2016, 2018; Berg, 2021). This dataset is part of the Fundamental Climate Data Record (FCDR) of brightness temperatures (T<sub>b</sub>) and provides, according to NASA, the best intercalibration of SSM/I sensors available (Berg et al., 2018). In the VODCA framework, we concatenate the VOD retrievals from SSM/I F8, F11, and F13 into a single record without further inter-calibration at the VOD level. As F8 and F11 do not overlap with each other or any other radiometer used in the VODCA framework, further intercalibration and validation steps are challenging. We mention that the patterns in VODCA CXKu are fully compliant with patterns observed in the single-frequency VODCA v1 Ku-band (Dorigo et al. (2021), Fig. SB2.6; Moesinger et al. (2020), Fig. 6), indicating they are not a result of combining multiple frequencies. There are no independent VOD datasets covering the period before 1992 that could serve as validation data. Additionally, all optical-based vegetation datasets available before 1992 are multi-sensor products, such as those using the Advanced Very High Resolution Radiometer (AVHRR) sensors onboard NOAA. These products are known to have calibration issues (Brown et al., 2006; Tian et al., 2015); therefore, their usage for this type of validation is questionable. In conclusion, we cannot exclude sensor intercalibration issues between SSM/I F08 and SSM/I F11. We will modify the text to make the users aware of this possible issue. Potential intercalibration issues between SSM/I F8 and F11 originate from the brightness temperature calibration and not from the VODCA framework.

To analyse the plausibility of the observed VODCA patterns, such as the decrease in 2003 and the increase in 2012, we computed global time series of yearly fAPAR (Fig. 2), as well as a Hovmoeller

diagram of monthly fAPAR anomalies (Fig. 3) using MODIS fAPAR data (Myneni and Park, 2021), which is a single-sensor dataset. We can observe a decrease in global yearly fAPAR in 2003 and an increase in 2012. Similar patterns can be observed in the Hovmoeller diagram, particularly in the Southern Hemisphere. Additionally, these patterns of decrease in 2003 are even more visible in the Hovmoller plot showing MODIS LAI anomalies, presented in (Moesinger et al., 2020) in Fig. 6. We therefore strongly believe that the patterns mentioned by the reviewer are plausible and we attribute them to natural variability.

*We replace the anomaly hovmoeller from the paper with Fig. 1. Fig. 2 is added to the Annex. SSM/I information on brightness temperature calibration is added to Chapter 2.1.2 "Passive microwave data". Information about the concatenation of SSM/I is added to Chapter 3.2 "Preprocessing". The patterns mentioned by the reviewer (1992, 2003, 2012) are discussed in Chapter 4.2 "Spatio-temporal consistency". We mention that we cannot exclude an intercalibration issue between F08 and F11 in Chapter 4.2 "Spatio-temporal consistency" and in Chapter 5 "Conclusion".*

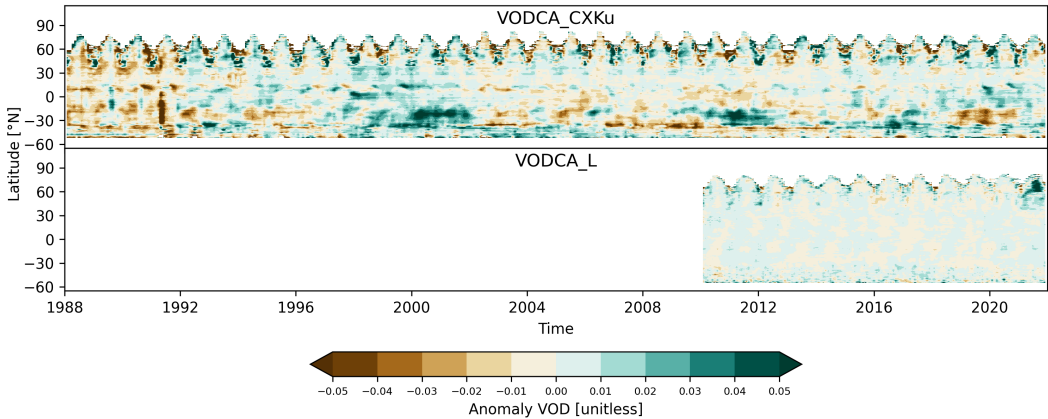


Figure 1: Hovmöller diagrams showing anomalies of the monthly means per latitude for VODCA CXXu and VODCA L. Anomalies have been computed as deviations from the climatology of the periods 1990 - 2020 (VODCA CXXu) and 2010 - 2021 (VODCA L).

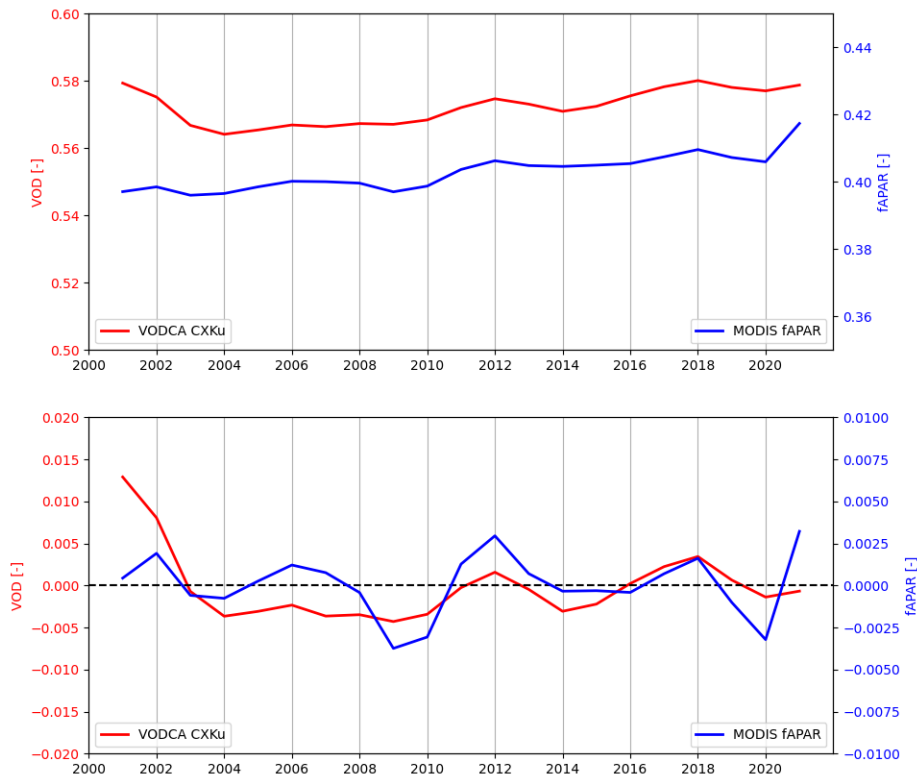


Figure 2: Yearly global time-series of VODCA CXXu and fAPAR for the bulk signal (upper graphic) and for anomalies (lower graphic).

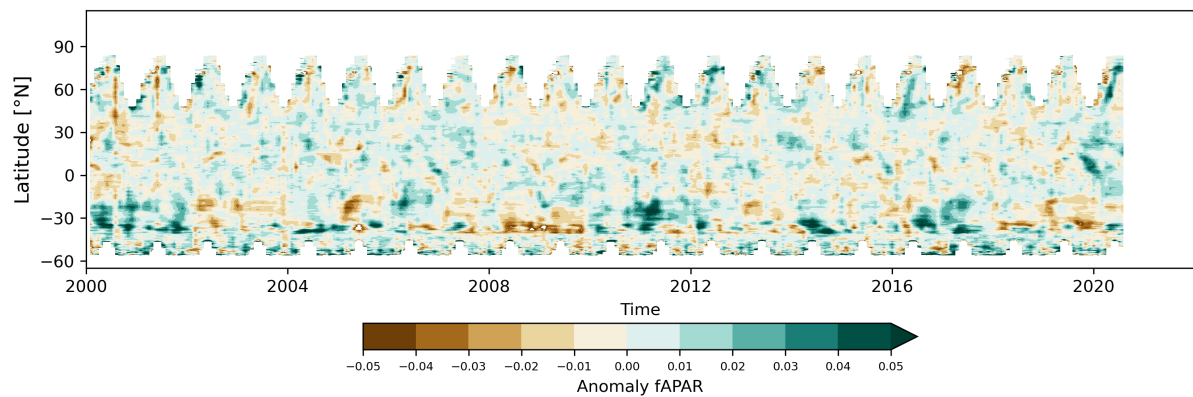


Figure 3: Hovmöller diagram showing anomalies of the monthly means per latitude for MODIS fAPAR. Anomalies have been computed as deviations from the long-term climatology (2000 - 2020).

## References

- Berg, W.: GPM SSM/I on F08 Common Calibrated Brightness Temperatures L1C 1.5 hours 13 km V07, Greenbelt, MD, USA, Goddard Earth Sciences Data and Information Services Center (GES DISC), 2021.
- Berg, W., Bilanow, S., Chen, R., Datta, S., Draper, D., Ebrahimi, H., Farrar, S., Jones, W. L., Kroodsmas, R., McKague, D., et al.: Intercalibration of the GPM microwave radiometer constellation, *Journal of Atmospheric and Oceanic Technology*, 33, 2639–2654, 2016.

- Berg, W., Kroodsmā, R., Kummerow, C. D., and McKague, D. S.: Fundamental climate data records of microwave brightness temperatures, *Remote Sensing*, 10, 1306, 2018.
- Brown, M. E., Pinzón, J. E., Didan, K., Morisette, J. T., and Tucker, C. J.: Evaluation of the consistency of long-term NDVI time series derived from AVHRR, SPOT-vegetation, SeaWiFS, MODIS, and Landsat ETM+ sensors, *IEEE Transactions on geoscience and remote sensing*, 44, 1787–1793, 2006.
- Dorigo, W., Mösinger, L., van der Schalie, R., Zotta, R.-M., Scanlon, T. M., and De Jeu, R.: Long-term monitoring of vegetation state through passive microwave satellites [in” State of the Climate in 2020”], *Bulletin of the American Meteorological Society*, 102, S110–S112, 2021.
- Moesinger, L., Dorigo, W., de Jeu, R., van der Schalie, R., Scanlon, T., Teubner, I., and Forkel, M.: The global long-term microwave vegetation optical depth climate archive (VODCA), *Earth System Science Data*, 12, 177–196, 2020.
- Myneni, R. and Park, T.: MODIS/Terra+ Aqua Leaf Area Index/FPAR 4-Day L4 Global 500 m SIN Grid V061, The Land Processes Distributed Active Archive Center (LP DAAC): Sioux Falls, SD, USA, 2021.
- Tian, F., Fensholt, R., Verbesselt, J., Grogan, K., Horion, S., and Wang, Y.: Evaluating temporal consistency of long-term global NDVI datasets for trend analysis, *Remote Sensing of Environment*, 163, 326–340, 2015.